Acta Cryst. (1977). A33, 663–667

Magnetic Structure of Fe_2WO_6, a Neutron Diffraction Study

BY H. PINTO AND M. MELAMUD

Department of Physics, Nuclear Research Center, Negev, PO Box 9001, *Beer Sheva, Israel*

AND H. SHAKED

Department of Physics, Nuclear Research Center, Negev, PO Box 9001, *Beer Sheva, Israel and Department of Physics, Ben Gurion University of the Negev, PO Box* 2513, *Beer Sheva, Israel*

(*Received* 19 *October* 1976; *accepted* 9 *December* 1976)

The structure of the compound Fe_2WO_6 is of the tri-α-PbO_2 type, and it belongs to the crystallographic space group *Pbcn* (D_{2h}^{14}). The lattice constants are $a=4{\cdot}576$, $b=16{\cdot}766$ and $c=4{\cdot}967$ Å, with four formula units per lattice point. Neutron ($\lambda\sim2{\cdot}4$ Å) diffraction patterns were taken at 300, 170, 77 and 4·2 K. Some intensity–temperature curves were also taken. The results may be summarized as follows. (1) The room-temperature pattern agrees with the reported X-ray determination of the crystallographic structure and ion positions. (2) Reflexions with $h+k$ odd not allowed by *Pbcn*, {010}, {030}, {100}, {031}, appear, on cooling, at $T_1\sim240$ K and increase in intensity down to liquid-helium temperature. (3) Reflexions with $h+k$ even, allowed by *Pbcn*: {020}, {021}, {040}, {110}, {111}, {150}, show, on cooling, an increase in intensity starting at $T_2\sim150$ K. The first set of reflexions is consistent with Cz^+, *i.e.* ferromagnetic (100) planes coupled antiferromagnetically with spin along [001]. This structure belongs to *Pbc'n'*. The space group *Pbc'n'*, however, allows the modes Cz^+ and Fx^+ or Cz^+ and Fx^- which is equivalent to a spin component along [100]. The second set of reflexions is consistent with Fx^+ and/or changes in the ion positions.

I. Introduction

The compound Fe_2WO_6 is the prototype of a new structural type called tri-α-PbO_2 (Senegas & Galy, 1974). The unit cell contains four formula units and the lattice constants are $a=4{\cdot}576$, $b=16{\cdot}766$ and $c=4{\cdot}967$ Å. The structure belongs to the orthorhombic space group *Pbcn* (D_{2h}^{14}). The ion positions are given in Table 1. The structure consists of zigzag chains of MO_6 ($M=$Fe or W) octahedra, sharing edges parallel to **c**. There are two types of chains: *A*, containing Fe(1) ions only, *B*, containing alternately Fe(2) and W ions. A projection on the (001) plane of the Fe and W ions is given in Fig. 1(*a*). In the present work we report the results of a neutron diffraction study (powder sample) of the low-temperature magnetic structure of Fe_2WO_6. Our conclusions concerning the liquid-helium temperature magnetic structure are different from those published (Weitzel, 1976) during the preparation of this manuscript (see *Discussion*).

Table 1. *Ion positions in* Fe_2WO_6, *space group Pbcn*

Position	Coordinates	Ions
4(*c*)	$\pm(0,y,\frac{1}{4};\ \frac{1}{2},y+\frac{1}{2},\frac{1}{4})$	Fe(1), Fe(2), W
8(*d*)	$\pm(x,y,z;\ \frac{1}{2}+x,\frac{1}{2}+y,\frac{1}{2}-z;$ $\frac{1}{2}-x,\frac{1}{2}+y,z;\ -x,y,\frac{1}{2}-z)$	O(1), O(2), O(3)

II. Experimental

Neutron ($\lambda\sim2{\cdot}4$ A) diffraction patterns with a powder sample at 300 (room temperature, RT), 170, 77 (liquid-nitrogen temperature) and 4·2 K (liquid-helium temperature, LHeT) were obtained. The RT and LHeT patterns are shown in Fig. 2. All the reflexions observed in the RT pattern are in agreement with the reported (Senegas & Galy, 1974) lattice constants. In the LHeT pattern two types of changes from the RT pattern are observed. (1) The appearance of reflexions with $h+k$ odd (*o*) not allowed by *Pbcn*, {010}, {030}, {100} and {031}. (2) The increase in intensity of reflexions with

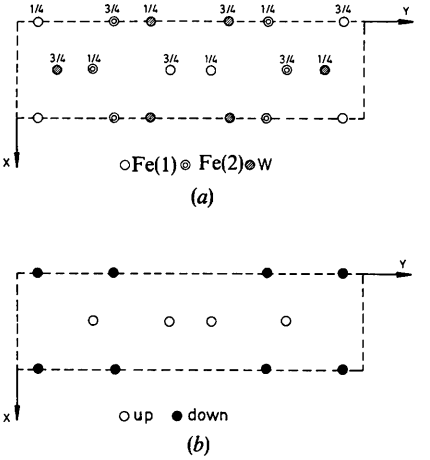

Fig. 1. Projection of the iron and tungsten ions on the (001) plane. (*a*) The crystallographic structure; the *z* coordinate values are shown. (*b*) The magnetic structure, Cz^+; the direction of the magnetic moment is shown.

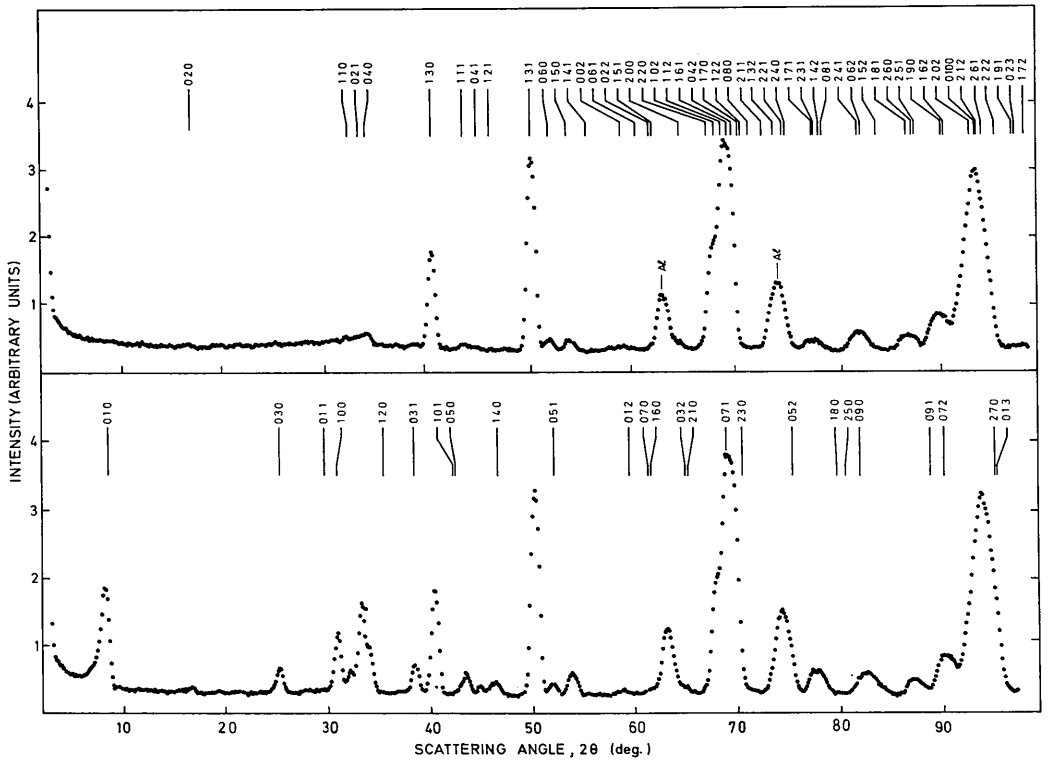

Fig. 2. Neutron ($\lambda \sim 2{\cdot}4$ Å) diffraction patterns of powder Fe_2WO_6. (*a*) At RT, indexing is according to the reflexions allowed by the space group *Pbcn*. (*b*) At LHeT, indexing of the additional reflexions is according to the magnetic space group *Pbc'n'*.

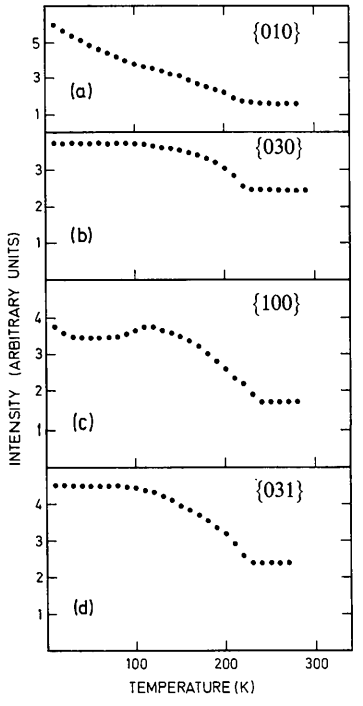

Fig. 3. Peak intensity–temperature curve of the reflexions {010}, {030}, {100}, {031}.

$h+k$ even (*e*) allowed by *Pbcn*, {020}, {021}, {040}, {111}, {150}. The peak intensity–temperature curves of the reflexions {010}, {030}, {100} and {031} are shown in Fig. 3. The reflexions exhibit a transition temperature $T_1 \sim 240$ K. The peak intensity–temper-

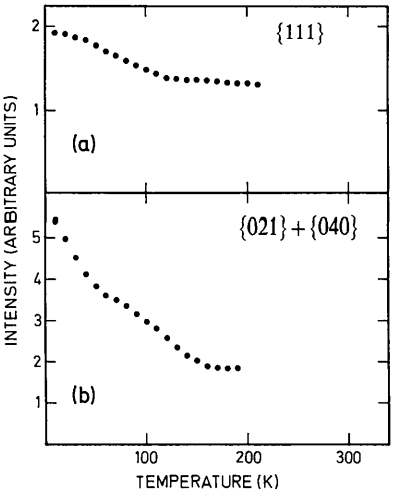

Fig. 4. Peak intensity–temperature curve of the lines {021}+{040} and {111}.

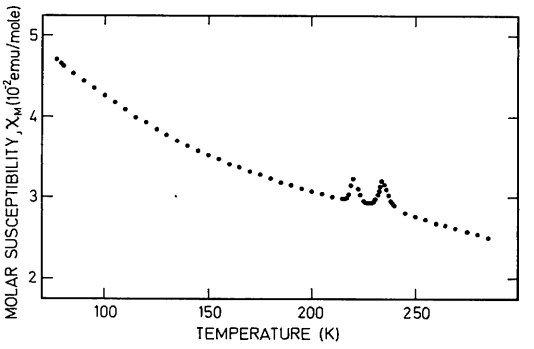

Fig. 5. Magnetic susceptibility temperature curve of powder Fe_2WO_6.

ature curves of the lines $\{021\}+\{040\}$ and $\{111\}$ (the rest of the lines were too weak to be studied) are shown in Fig. 4. The lines exhibit a transition temperature $T_2 \sim 150$ K. The diffraction patterns taken at 170 and 77 K (not shown) do not add any new information to those obtained from the LHeT pattern and intensity–temperature curves. The temperature dependence of the magnetic susceptibility was also measured. The resulting curve is shown in Fig. 5.

III. Crystallographic structure

Nuclear intensities were calculated for the structure which belongs to the space group *Pbcn*. Senegas & Galy (1974) mention the possibility of a mixture between the Fe(2) and W ions of chain *B*. The proposed mixture coefficient, *m*, was about 6%. The reported position parameters (Senegas & Galy, 1974)* without and with a mixture of ions are essentially the same.† The position parameters and the Debye–Waller constant, *B*, were refined to give a best fit (least squares) of the calculated to the observed integrated RT intensities for $0 \le m \le 50\%$. The corresponding weighted *R* values $(R=\{\Sigma[(I_o-I_c)/\sigma]^2/\Sigma(I_o/\sigma)^2\}^{1/2}$ where the σ's are estimated errors in I_o) and the position parameters are practically constant throughout this range of *m*. A mixture of the three ions, Fe(1), Fe(2) and W was also investigated and led to similar results. We therefore conclude that our data is not appropriate for the unambiguous determination of *m*. Hence our analysis will be based on the assumption that $m=0\%$. The calculated and the observed integrated intensities are given in Table 2. The intensities calculated with the reported position parameters are also given in Table 2. The corresponding position parameters and weighted *R* values are given in the next section (Table 5).

* The reported parameters were refined by Senegas & Galy using 828 independent reflexions collected by an X-ray diffractometer from a single crystal of Fe_2WO_6.

† The principal change was in the values of the Debye–Waller constants, B_i, of the different ions, *i.e.* the assumption was made in order to correct these values.

Table 2. *Comparison of calculated and observed integrated intensities at RT*

The calculated intensities were obtained with: (*a*) the reported parameters (Senegas & Galy, 1974), (*b*) the present-work parameters.

No.	{*hkl*}	$I_o \pm \sigma$	I_c (*a*)	I_c (*b*)
1	020	0± 200	196	129
2	110, 021, 040	4600± 250	2643	4483
3	130	17500± 200	18186	17590
4	111, 041	1200± 200	1215	1239
5	121	0± 200	6	13
6	131	42700± 250	42687	42912
7	060	2200± 130	2236	2331
8	150	2300± 140	1217	2378
9	141	0± 200	20	60
10	002, 061	1600± 270	1245	1683
11	220, 102, 112, 161 042, 170, 122, 080	98300±1100	93771	93686
12	171, 231, 142, 081	3900± 750	4006	3431
13	241, 062, 152	7767± 940	7056	7581
14	181, 260, 251	6322± 770	6468	6734
15	190, 162, 202, 0100 212, 261, 222	119500±1680	123526	122836

IV. Magnetic structure

The magnetic character of the transition at T_1 is clearly shown in the magnetic susceptibility–temperature curve (Fig. 5). Although the origin of the second peak is not clear to us, it is safe to assume that a magnetic structure which appears below T_1 contributes to the *o* reflexions. The magnetic configuration which is consistent with the *o* reflexions is C^+ (Gurewitz & Shaked, 1972). The notation *C* applies to a set of four equivalent ions, *i.e.* Fe(1) or Fe(2). Choosing the ions situated at $(0,y,\frac{1}{4})$ as the first of the sequence we define C^+ for $C[\text{Fe}(1)]+C[\text{Fe}(2)]$ and C^- for $C[\text{Fe}(1)]-C[\text{Fe}(2)]$. The magnetic structure factor of the reflexions *h*00, is independent of *y* and equals zero for the C^- mode. The non-zero intensity of the {100} line excludes therefore this possibility. The only maximal symmetry magnetic structure which contributes to {100} is hence equal to the Cz^+ mode. This structure consists of ferromagnetic (100) planes, coupled antiferromagnetically with spins along [001] (Fig. 1*b*), and it belongs to the magnetic space group *Pbc'n'*. This space group allows also a spin component along the *x* axis, *i.e.* Fx^+ for $Fx[\text{Fe}(1)]+Fx[\text{Fe}(2)]$ and Fx^- for $Fx[\text{Fe}(1)]-Fx[\text{Fe}(2)]$. These modes can contribute only to the nuclear reflexions, *i.e.* to the reflexions allowed by *Pbcn*. As stated in §III our data is not appropriate for the unambiguous determination of the mixture coefficient *m*. To assume $m \neq 0$ and apply it to the magnetic structure will introduce an additional ambiguity. Four magnetic structures were consequently considered for $m=0$:

(1) Cz^+, $\mu[\text{Fe}(1)]=\mu[\text{Fe}(2)]$,
(2) Cz^+,
(3) Cz^+ and Fx^+ or Fx^-, $\mu[\text{Fe}(1)]=\mu[\text{Fe}(2)]$,
(4) Cz^+ and Fx^+ or Fx^-.

The position parameters and the values of the magnetic moments μ(Fe) were refined to give a best fit (least squares) of the calculated to the observed integrated

Table 3. *The magnetic moments, in Bohr magnetons, for the four magnetic structures considered and their corresponding weighted R values*

	1	2	3	4
μ_x[Fe(1)]	0	0	1·4±0·7	0·85±0·7
μ_z[Fe(1)]	2·48±0·07	2·55±0·07	2·55±0·15	2·66±0·07
μ_x[Fe(2)]	0	0	1·4±0·7	0±0·5
μ_z[Fe(2)]	2·48±0·07	2·15±0·15	2·55±0·15	1·96±0·15
R %	7·3	6·5	9·3	6·4

Table 4. *Comparison of calculated and observed integrated intensities at LHeT*

The calculated intensities were obtained with: (*a*) The present-work parameters for the magnetic structure, Cz^+, shown in Fig. 1(*b*) with the constraint μ[Fe(1)] = μ[Fe(2)]. (*b*) The present-work parameters for the same magnetic structure without the constraint.

No.	{*hkl*}	$I_o \pm \sigma$	I_c (*a*)	I_c (*b*)
1	010	26300± 850	23155	26136
2	020	1000± 350	1840	1730
3	030	4100± 450	4078	3713
4	011	0± 300	179	107
5	100	10600± 450	11734	10612
6	110	3400± 250	2958	3014
7	021, 040	22500± 600	21159	21292
8	120	0± 300	210	27
9	031	5000± 470	4805	4321
10	130	18700± 490	19706	19628
11	101, 050, 111	3300± 500	3202	2882
12	041	1100± 400	1433	1336
13	121, 140	2600± 400	4480	4160
14	131	43900± 650	46457	46260
15	060, 051	1500± 350	1257	1185
16	150	4900± 460	5132	5352
17	141	0± 300	244	378
18	002, 012, 061	1100± 780	2223	2129
19	220, 102, 112, 071, 161 042, 170, 230, 122, 080	111700±1300	105520	105350
20	171, 231, 142, 081, 180	9300± 730	10578	10220
21	250, 090, 241, 062, 152	10100±1000	13309	13288
22	181, 260, 251	5700± 680	3940	3568
23	091, 190, 072, 162, 202, 0100 212, 261, 003, 270, 222, 013	131200±1680	132560	132930

LHeT intensities. The refined magnetic moment with the corresponding weighted R values are given in Table 3. Sign μ_x[Fe(1)] = sign μ_x[Fe(2)] is equivalent to Fx^+. We conclude that the magnetic structure is essentially Cz^+ possibly with a weak Fx^+ while the magnetic moments of the ions can be slightly different [structure (4)]. The calculated intensities for the magnetic structure Cz^+ without and with the constraint, μ[Fe(1)] = μ[Fe(2)] and the observed integrated LHeT intensities are given in Table 4. The corresponding position parameters and magnetic moments are given in Table 5.

V. Summary of results

The previously determined (with X-rays) RT crystallographic structure (Senegas & Galy, 1974) is confirmed (with neutrons). Two transition temperatures, $T_1 \sim 240$ K and $T_2 \sim 150$ K, are observed. The first transition at T_1 is due to a magnetically ordered Cz^+Fx^+ structure whereas the second transition at T_2 is crystallographic (shift of positions) in character.* [There is no evidence of T_2 in the magnetic susceptibility–temperature curve (Fig. 5).] The magnetic structure at LHeT with corresponding shifts in the ion positions was determined. The structure found is essentially Cz^+ with possibly weak Fx^+. The anomaly in the magnetic susceptibility (second peak) and the unusual intensity–temperature curves remain without an explanation.

VI. Discussion

The magnetic structure proposed by Weitzel (1976) for Fe_2WO_6, has the same z-component ordering as given

* It must be stated that the contribution of Fx^+ to the intensities of the nuclear reflexions is negligible and the increase in intensity of the reflexions is essentially due to the shift of ionic positions.

Table 5. *Ionic parameters of* Fe_2WO_6 *at RT and LHeT*

(*a*) With the constraint μ[Fe(1)] = μ[Fe(2)].
(*b*) Without the constraint.

	RT		LHeT	
	Reported*	Refined†	(*a*)	(*b*)
μ[Fe(1)]	—	—	2·48 ±0·07	2·55 ±0·07
μ[Fe(2)]	—	—	2·48 ±0·07	2·15 ±0·15
y[Fe(1)]	0·0564	0·061±0·001	0·064±0·002	0·064±0·002
y[Fe(2)]	−0·2758	−0·279±0·001	−0·283±0·003	−0·284±0·003
y(W)	0·38725	0·386±0·001	0·362±0·003	0·361±0·002
x[O(1)]	0·2400	0·240±0·002	0·235±0·005	0·236±0·005
y[O(1)]	0·0409	0·039±0·001	0·029±0·004	0·030±0·004
z[O(1)]	0·5958	0·590±0·007	0·56 ±0·02	0·56 ±0·02
x[O(2)]	0·2734	0·270±0·002	0·257±0·005	0·254±0·005
y[O(2)]	0·1271	0·125±0·001	0·125±0·002	0·125±0·002
z[O(2)]	0·0692	0·090±0·005	0·136±0·009	0·135±0·008
x[O(3)]	0·2760	0·275±0·002	0·247±0·007	0·244±0·007
y[O(3)]	0·2035	0·204±0·001	0·217±0·003	0·215±0·003
z[O(3)]	0·5817	0·587±0·007	0·557±0·013	0·554±0·013
B	0·27±0·38	0·30 ±0·18	0	0
R %	5·5	2·2	7·3	6·5

* Senegas & Galy (1974).
† Present work.

in Fig. 1(*b*) of this work (Cz^+). To allow for the observed intensity increase in the reflexions {021} and {040}, which are not allowed by Cz^+, Weitzel concludes that the magnetic structure at LHeT has an antiferromagnetic x component. This component causes a symmetry reduction, and the magnetic space group is $Pn'c2'$.

It was shown in this work that, allowing for small parameter changes (conforming with the RT space group *Pbcn*), the most probable structure is Cz^+ (space group $Pbc'n'$) with or without an x component of weak ferromagnetism, which is allowed by $Pbc'n'$. We propose this structure, using the established principle that the choice of the highest possible symmetry model is the logical choice (Cox, 1972).

The symmetry $Pbc'n'$ conforms also with the second-order phase-transition theory (Landau & Lifshitz, 1958; Mukamel, 1973). This theory in our case (orthorhombic symmetry, and no cell enlargement) allows only a symmetry reduction by a factor of two, through the loss of the time-inversion operator, as is the case with $Pbc'n'$ (whereas the reduction from *Pbcn* to $Pn'c2'$ is by a factor of four).

The reflexions {021} and {040} may include, according to this proposal, nuclear and ferromagnetic contributions (no contributions from Fe_2O_3 are detected in our patterns). A discrepancy in the intensity calculation of the reflexions {050} and {111} is not solved in Weitzel's work because these reflexions are not resolved in his pattern. These reflexions cannot be quantitatively resolved in our longer-wavelength pattern.

The authors are indebted to Professor S. Shtrikman of the Weizmann Institute of Science for providing the sample and for many helpful discussions. Discussions with Professor U. Atzmoni and Mr G. Dublon of this laboratory were much appreciated.

References

Cox, D. E. (1972). *IEEE Trans. Magn.* **8**, 161–182.
Gurewitz, E. & Shaked, H. (1972). *Limiting Conditions on Possible Reflexions from Magnetic Configurations in* D^i_{2h} $i=1,2\ldots16$. Report NRCN 316. Nuclear Research Center, Negev, Israel.
Landau, L. D. & Lifshitz, E. M. (1958). *Statistical Physics*, Ch. 14. New York: Addison Wesley.
Mukamel, D. (1973). *Symmetry Aspects of Phase Transitions*, Thesis, Weizmann Institute, Rehovot (unpublished).
Senegas, J. & Galy, S. (1974). *J. Solid State Chem.* **10**, 5–11.
Weitzel, H. (1976). *Acta Cryst.* A**32**, 592–597.

Acta Cryst. (1977). A**33**, 667–671

A General Property in Extinction Theories: the Relation between Incident Point Sources and Homogeneous Beams. Application to Mosaic and Perfect Crystals

By Pierre Becker

Centre de Mécanique Ondulatoire Appliquée, CNRS and Université Pierre et Marie Curie, 23 rue du Maroc, 75019 Paris, France

(*Received* 19 *November* 1976; *accepted* 25 *January* 1977)

The integrated reflectivity from an incident homogeneous beam (or plane wave) is shown to be a volume integral involving the intensity diffracted by a source point located on the surface of incidence of the crystal. Owing to the boundary conditions, the solution of the equations for extinction (either kinematical or dynamical) is often simpler with point sources than plane waves. The property that is established extends the domain of solution of diffraction theories: it is applied to mosaic-crystal equations and to the case of perfect crystals. In the latter case, a physically meaningful solution is found for primary extinction.

Introduction

Extinction can be treated through various models originating in either kinematical (intensity coupling) or dynamical (wave coupling) theories. Kato (1976) has partially reconciled the two approaches, solving Takagi's (1969) equations in a statistical way under definite conditions. For optical coherence length smaller than the extinction distance, he obtained intensity coupling equations which can be shown to be identical with those employed to describe mosaic theories (Becker, 1977). The solution to these equations has been looked for by Zachariasen (1967), Becker & Coppens (1974) and Werner (1974). Kato's demonstration is obtained *via* the relation that exists between spherical and plane-wave theories of diffraction.

Homogeneous beams (or plane waves) are of general use in diffractometry. It will be shown that the solution for any set of diffraction equations can be decomposed into the superposition of contributions from point sources that are located on the surface of the crystal. The integrated reflectivity is then transformed into a volume integral, where the function to be integrated is the intensity diffracted by a point source associated with the variable point in the crystal.

The method will be then applied to mosaic and